A Wireless Transient Attenuated-exponential Overpressure Beamforming with for Far-field Blast Source Localization

Shang Gao, *IEEE Member,* Zirui Zhang, Yan Zong, *IEEE Member,* Guiyun Tian, *IEEE Senior Member,* Xuewu Dai, *IEEE Senior Member,* Yongteng Zhong, Xin Jin

***Abstract*—Time-domain beamforming is more suitable for blast wave transient signal than frequency-domain beamformer because wide-band spectrum of noise makes the beamforming image less clear. To avoid the gust effects and enable the location of blast source accurately, this paper proposes a new one-dimensional Far-field delay-and-sum (DAS) beamforming method with an attenuate exponential function model for wireless overpressure transient signal. In addition, we also design wireless overpressure peak and root-mean-square (RMS) directional estimators to assess the performance of the proposed new DAS beamforming method. Furthermore, the effects of the wireless pressure sensor node (WPSL) spacing, the number of WPSLs and side lobe level brought from noise on the beam width are investigated in the two estimators. The proposed formula is verified by a uniformly spaced linear sensing array, and the results verify the feasibility of the proposed method in blast source localization. This paper is conducted to provide new insight into blast source localization algorithm, and further open a door for transient blast overpressure source localization scenarios in future.**

***Index Terms*—Time Beamforming, Delay-and-sum, Blast wave, WSN, Source localization, Overpressure**

I. Introduction

AIR explosions in defense and civil applications demands for high-precision and ease-deployed sensors for overpressure measurement in air blast [1]. Blast damage effectiveness evaluation relies on the comparison between accurate experimental data and the dynamic parameters measurement (e.g. peak overpressure, positive impulse, and the duration of the positive phase) with theory models or numerical simulations [2]. Nowadays, most cables for the blast wave measurement in air blast experiment are time-consuming manpower and labor-extensive, easily leading to operational problems or electrical failure such as short-circuits or electrical breakdowns before the experiment process [3, 4]. To handle with these issues, some new alternative approaches based on wireless sensor network have applied in blast wave monitoring in recent years [5-9].

The overpressure transient signal is the most important dynamic parameter to be measured for evaluating the mass and power of TNT explosion [10-12]. Thus, it is meaningful to reconstruct or multiple dimensional overpressure data model for shock wave in blast field [13, 14]. However, the localization of blast source should be implemented in advance before the overpressure spatial reconstruction, because the precision of reconstruction method highly relies on the blast source position accuracy [15]. As the static explosion in the ground, the localization of blast source is almost identified [16]. On the other hand, in many blast applications such as underwater torpedoes explosion under ocean waves, air rocket boosters, dynamic blast in the air ammunition, the initial zero time of the blast is unknown which contributes to localize the accurate position of blast source difficultly. Therefore, it is vital to develop a specific time-domain beamformer method for blast source localization.

Sound localization approaches is first introduced in world war I for finding enemy weapons [17]. Now, it can be divided into three types: time of arrival (TOA), time difference of arrival (TDOA), angle of arrival (AOA) [18]. They have been widely used in underwater object target [19], weapon system classification [20], gun shooter localization [21], oil leakage[22] and counter-sniper localization [23, 24]. However, the common drawbacks of these methods are the multiple intersections between two signal localization hyperbolas despite a single-point source[25]. The frequency-domain and time-domain beamforming are another powerful methods which have more effective for localize the direction of blast source by enhancing a desired signal component and reducing undesired noise. Till now, in radar, telecommunication, sonar and biomedical applications, many beamforming methods have been widely applied [26-28]. The former relying on Fourier transform adopts the sensor data to search the source direction angle. The method estimates the direction by finding the maximum beamforming power through a weighting function. In addition, the latter is on the basis of a time-domain DAS beamformer. So far, sound localization for blast source is widely applied. However, the sound localization is seriously and easily influenced by the wind [20]. To avoid gust effects in real field application, it is an alternative approach to achieve the blast source localization by overpressure signal which is also viewed as only one approach to evaluate indicator for the power of TNT explosion [29]. In addition, the supersonic speed of

This work was supported in part by Nanjing University of Science and Technology under Research Start-Up Funds under Grant AE89991/032, in part by the Fundamental Research Funds for the Central Universities under Grant 309181A8804 and Grant 30919011263, in part by Natural Science Foundation of Jiangsu Province, China under Grant BK20190464, in part by Jiangsu Planned Projects for Postdoctoral Research Funds under Grant 1003-YBA20012, in part by Chinese Postdoctoral Science Foundation under Grant 2020M671481.

This article has been accepted for publication in IEEE Sensors Journal. This is the author's version which has not been fully edited and content may change prior to final publication. Citation information: DOI 10.1109/JSEN.2022.3187762

shock wave is higher than that of sound, which indicates that the arrival time of shock wave is ahead of sound. Thus, as for arrival time from signal extraction, it may be more precise for blast source localization by using overpressure signal. In addition, it is expensive and unpractical that both the pressure sensors and acoustic sensors are deployed in real blast monitoring application [30]. Thus, we should develop the beamforming method only depending on overpressure signal to localize the blast source and evaluate the power of TNT explosion simultaneously.

As a transient signal, the overpressure signal of blast wave is completely different form blast sound, guided wave or electromagnetic wave in terms of wave function model, wave frequency and wave speed [31]. Especially, the distinct difference between them is that the sound source model adopts triangular pulse function while blast overpressure signal is modeled as attenuate exponential function, which makes the beamformer methods for them quite different. It is unknown whether the various existing traditional or improved beamforming methods are appropriate or effective for blast source localization. Thus, it is necessary and interesting to explore some fundamental beamforming methods based on overpressure signal for blast source localization and further investigations of more far-field localization methods in future. In this paper, the main contributions can be summarized as follows:

1) We propose a new overpressure localization approach in comparison with the traditional sound localization for blast source position. The proposed method only depending on overpressure signal is able to localize the blast source and evaluate the power of TNT explosion simultaneously.

2) To our best knowledge, this is an attempt to propose a fundamental time-domain DAS beamforming with attenuate exponential function for peak and RMS estimation in overpressure transient signal, providing new insights for frequency-domain and spatial-domain blast source localization algorithms.

The paper proposes a new overview for the solution for far-field blast source localization by overpressure estimation based on time-domain beamforming method. The article is organized as follows. The problem statements of are presented in Section II. In addition, the peak and RMS estimators for the blast wave source localization are proposed in Section III. In order to verify the performance of proposed time-domain DAS beamforming method, the comparisons between RMS and peak estimators in terms of WPSL spacing, the number of WPSL, source direction angle and noise are implemented in air blast field test in Section IV. Lastly, we conclude the work and discuss future work in Section V.

II. The Problem Statements

In the blast source localization, the M-element uniform ground linear wireless array measure the blast wave signal, as shown in Fig.1 (a). Due to the different distances between each WPSL and the blast source, the propagation time of blast wave varies as arriving at each WPSL. As the blast source is located from pressure sensing array in far-field, we can assume that the source wave identification is the planar wave fronts. Thus, the reaching time of blast wave for one WPSL located at the distance D away from the blast source is defined as:

$$t_s = D\cos\theta_s / c \tag{1}$$

Where c is the speed of blast wave, θ_s is the blast source direction. Thus, the measured signal at the WPSL is also denoted as:

$$S_i(t) = s(t-a-(i-1)\tau_s) + n_i(t) \tag{2}$$

Where i is the index of each WPSL ($i = 1, 2, ..., N$), $s(t)$ is the signal of the blast wave arriving at the WPSL and the a is the time delay from the first WPSL to the blast source. In addition, the zero-mean Gaussian noise $n_i(t)$ irrelevant with the source $s(t)$ is considered in the final signal $S_i(t)$. τ_s is time delay between two adjacent WPSLs.

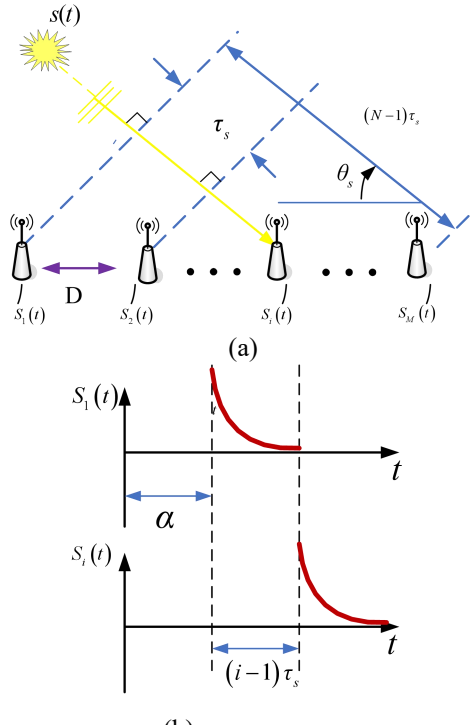

Fig. 1. (a) Uniform linear array under incident planar waves; (b) overpressure signals in the time-domain at two different WPSL.

To compensate the time difference of different WPSLs, the DAS beamformer method employs an predefined delay time to the signal of each WPSL. In the far-field, all delayed signal are summed together to generate the final output of beamformer method in terms of the steering angle θ which is denoted as:

$$b(\theta,t) = \frac{1}{N}\sum_{i=1}^{N} S_i(t+(i-1)\tau) \tag{3}$$

Where τ is the time delay calculated as $D\cos\theta / c$.

The predefined time delay relies on the steering angle θ. The Eq. (4) can be redefined by substituting Eq.(2) into Eq. (3) :

$$b(\theta,t) = \frac{1}{N}\sum_{i=1}^{N} s(t-a-(i-1)(\tau_s-\tau)) + \frac{1}{N}\sum_{i=1}^{N} n_i(t+(i-1)\tau) \tag{4}$$

III. The Model of Blast Wave Source Localization

A. The peak and RMS estimators for blast wave source localization

The Eqs.(4) provides the approach for evaluating the performance and ability of time-domain beamformer with

regards to the beamwidth and side lobe level in a noisy environment. To localize the direction of actual source, the beamforming power in all directions should be calculated. If the energy power of Eqs. (4) reaches the maximum value, the trial source direction is the actual source direction $\theta = \theta_s$. To evaluate the performance of the time-domain beamformer, different the directional estimators have been defined. The typical estimator, the root-mean-square (RMS) of $b(\theta,t)$ can be defined as:

$$b_{rms}(\theta,\triangle T)=\sqrt{\frac{1}{\triangle T}\int_{t_0}^{t_0+\triangle T}\left[b(\theta,t)\right]^2 dt} \tag{5}$$

where $\triangle T$ is the time duration of the output and the transient blast event occurs during the time $[t_0, t_0+\triangle T]$. As another estimator, the peak value of $b(\theta,t)$ is denoted as:

$$b_{peak}(\theta)=\max_t\left[\left|b(\theta,t)\right|\right] \tag{6}$$

In addition, the estimated blast source directions by the RMS estimators and peak estimators are defined as follows:

$$\hat{\theta}_{rms}=\arg\max_{\theta\in[0,\pi]}\left[b_{rms}(\theta,\triangle T)\right] \tag{7}$$

$$\hat{\theta}_{peak}=\arg\max_{\theta\in[0,\pi]}\left[b_{peak}(\theta)\right] \tag{8}$$

B. The implementation of the time-domain beamforming method for overpressure transient signal

The fundamental overpressure signal model of blast wave is demonstrated in Fig.2. The dynamic parameters of the blast wave are determined by the records of pressure vs. time history. We consider an attenuate exponential function as the model of the overpressure signal with the time duration ε for the overpressure signal:

$$P_i(t)=Ae^{-b(t-c)} \tag{9}$$

Where A is the peak value of overpressure, b and c are constant value. In far-field, the b and A is the same for each WPSL.

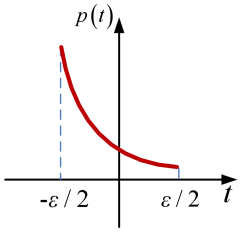

Fig.2 Attenuate exponential function modeling for overpressure signal

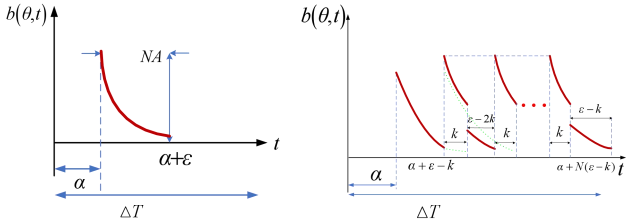

(a) (b)

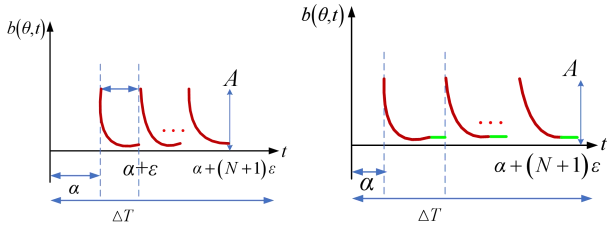

(c) (d)

Fig.3. Proposed beamformer outputs in various steering angles at (a) $\cos\theta = 0(\theta=\theta_s=90^\circ)$, (b) $|\cos\theta| = \varepsilon c / D$, (c) $0<|\cos\theta|<\varepsilon c / D$, and (d) $|\cos\theta| > \varepsilon c / D$

As for the RMS estimation with the time duration ε, the power of an attenuate exponential signal function is calculated as:

$$b_{rms}^2(\theta,\triangle T)=\frac{1}{\triangle T}\int_{t_0}^{t_0+\triangle T}\left[P_i(\theta,t)\right]^2 dt=\frac{1}{\Delta T}\int_{-\varepsilon/2}^{\varepsilon/2}p_i^2(t-c)dt$$
$$=\frac{N^2A^2}{\varepsilon}\int_{-\varepsilon/2}^{\varepsilon/2}e^{-2b(t-c)}dt=\frac{N^2A^2}{-2b\varepsilon}\left(e^{-2bt+2bc}\right)\Big|_{-\varepsilon/2}^{\varepsilon/2}=\frac{N^2A^2e^{bc-ba}}{2b\varepsilon}(1-e^{-2b\varepsilon}) \tag{10}$$

Where N is the number of WPSL, D is the WPSL spacing, 2ε is the time duration of the blast source, A is the amplitude of attenuate exponential signal function, α is the time delay between the blast source and the first WPSL S_1, c is the speed of blast wave, θ_s is the incident angle of a plane wave. If the signal with zero-mean white Gaussian noise $n_j(t)$ has noise variance σ^2. The power of $n_j(t)$ can be define as:

$$E[n_j^2(t)]=\sigma^2 \tag{11}$$

where $E[\bullet]$ is the expectation operator. Thus, according to Eqs. (10) and Eqs. (11), the signal-to-noise ratio (SNR) of the input overpressure signals can be defined as:

$$SNR_{input}=\frac{N^2A^2e^{bc-ba}}{2b\varepsilon\sigma^2}(1-e^{-2b\varepsilon}) \tag{12}$$

If the oriented angle between the blast source and M-element uniformly ground linear wireless array is 90° under noise-free conditions, the Eqs. (4) can be organized into four cases. As shown in Fig. 3(a), if redefined delay for each WPSL is identical to the source direction θ_s, the overpressure signal of each WPSL adds up to $t=\alpha$. Thus, the maximum values of RMS and peak are calculated as:

$$b_{rms}(\theta)\Big|_{\theta=\theta_s}==NAe^{bc-ba}\sqrt{\frac{1-e^{-2b\varepsilon}}{2b\varepsilon}} \tag{13}$$

$$b_{peak}(\theta)\Big|_{\theta=\theta_s}=NA \tag{14}$$

Eqs. (13) indicates that the RMS value is small as ε is large and the blast source is steep. Additionally, the delay-and-sum beamformer is steered into the direction $\theta\neq\theta_s$ are shown in Fig.3(b)-(d). In Fig. 3(b), the attenuate exponential function in each WPSL overlap and are summed to $|D\cos\theta|/c=\varepsilon$. In this respect, the RMS output is defined as:

This article has been accepted for publication in IEEE Sensors Journal. This is the author's version which has not been fully edited and content may change prior to final publication. Citation information: DOI 10.1109/JSEN.2022.3187762

$$b_{rms}(\theta)\Big|_{|d\cos\theta|/c=\varepsilon}=\sqrt{\frac{1}{N(\varepsilon-k)}[\int_{a}^{a+\varepsilon-k}b^2(t-c)+\int_{a+\varepsilon-k}^{a+\varepsilon}\left[b(t-c)+b(t-c-\varepsilon+k)\right]^2}$$

$$+\int_{a+\varepsilon}^{a+2\varepsilon-2k}b^2(t-c-\varepsilon+k)dt+\int_{a+2\varepsilon-2k}^{a+2\varepsilon-k}b(t-c-\varepsilon-k)b(t-c-2\varepsilon+2k)\cdots\cdots]$$

$$=A\sqrt{\frac{(N+1)e^{-2b(a-c)}}{2bN(k-\varepsilon)}(1-e^{-2b\varepsilon})+\frac{e^{2bc-2ba-b\varepsilon-bk}}{b(k-\varepsilon)}(1-e^{-2bk})} \quad (15)$$

In the respect, the power of noise is defined as:

$$E\left[\left(\frac{1}{N}\sum_{j=1}^{M}n_j(t+(j-1)\tau_s)\right)^2\right]=\frac{\sigma^2}{N} \quad (16)$$

leading to the output SNR of Eqs.(15):

$$SNR_{input}=\frac{N(N+1)A^2e^{-2b(a-c)}}{2bN(k-\varepsilon)\sigma^2}(1-e^{-2b\varepsilon})+\frac{NA^2e^{2bc-2ba-b\varepsilon-bk}}{b(k-\varepsilon)\sigma^2}(1-e^{-2bk}) \quad (17)$$

The peak value of output is defined as:

$$b_{peak}(\theta)\Big|_{|d\cos\theta|/c=\varepsilon}=A(e^{k+c-\varepsilon}+e^{-c}) \quad (18)$$

In Eqs.(13) and Eqs.(18), $b_{peak}(\theta)$ has a constant value for $|d\cos\theta|/c>\varepsilon$. Fig.3(c) and Fig.3(d) show multiple attenuate exponential signals separate from each other. The output RMS value is a constant as $|D\cos\theta|/c>\varepsilon$ and is calculated as:

$$b_{rms}(\theta)\Big|_{|d\cos\theta|/c\geq\varepsilon}=\sqrt{\frac{1}{\Delta T}\int_{a}^{a+(N+1)\varepsilon}b^2(t)dt}=\sqrt{\frac{1}{\Delta T}[\int_{a}^{a+\varepsilon}b^2(t-c)dt+}$$

$$\int_{a+\varepsilon}^{a+2\varepsilon}b^2(t-c-\varepsilon)dt++\int_{a+(N-1)\varepsilon}^{a+N\varepsilon}b^2(t-c-N\varepsilon+\varepsilon)dt]$$

$$=\sqrt{\frac{A^2}{\varepsilon}(\int_{a}^{a+\varepsilon}e^{-2b(t-c)}dt+\int_{a+\varepsilon}^{a+2\varepsilon}e^{-2b(t-c-\varepsilon)}dt+\ldots+\int_{a+(N-1)\varepsilon}^{a+N\varepsilon}e^{-2b(t-c-N\varepsilon+\varepsilon)}dt)}$$

$$=Ae^{-b(a-c)}\sqrt{\frac{N(1-e^{-2b\varepsilon})}{2b\varepsilon}} \quad (19)$$

leading to the output SNR of Eqs. (18):

$$SNR_{input}=\frac{N^2A^2e^{-2b(a-c)}(1-e^{-2b\varepsilon})}{2b\varepsilon\sigma^2} \quad (20)$$

In this respect, the peak output is defined as:

$$b_{peak}(\theta)\Big|_{|d\cos\theta|/c>\varepsilon}=A \quad (21)$$

The each output normalization of the RMS by maximum value is defined as $b_{rms}(\theta)\Big|_{\theta=\theta_s}$ in the time duration of ΔT. As a result, the Eqs. (13), (15) and (19) can be defined as:

$$\frac{b_{rms}(\theta)}{b_{rms}(\theta)\Big|_{\theta=\theta_s}}=\begin{cases}1 \quad for\left|D\cos\theta\right|/c=0\\ [\sqrt{\frac{(N+1)\varepsilon}{N(k-\varepsilon)}+\frac{1-e^{-2bk}}{1-e^{-2b\varepsilon}}\cdot\frac{2\varepsilon}{k-\varepsilon}\cdot e^{-b\varepsilon-bk}}/N,1] \quad for 0<\left|D\cos\theta\right|/c<\varepsilon\\ [1/\sqrt{N},1/\sqrt{\frac{(N+1)\varepsilon}{N(k-\varepsilon)}+\frac{1-e^{-2bk}}{1-e^{-2b\varepsilon}}\cdot\frac{2\varepsilon}{k-\varepsilon}\cdot e^{-b\varepsilon-bk}}/N] \quad \text{otherwise}\end{cases} \quad (22)$$

The each output normalization of the peak estimator by maximum value is defined as $b_{peak}(\theta)\Big|_{\theta=\theta_s}$ in the time duration of ΔT. As a result, the Eqs. (14), (18), (21) can be defined as:

$$\frac{b_{peak}(\theta)}{b_{peak}(\theta)\Big|_{\theta=\theta_s}}=\begin{cases}1 \quad for\left|D\cos\theta\right|/c=0\\ [(e^{k+c-\varepsilon}+e^{-c})/N,1] \quad for\left|D\cos\theta\right|/c\leq\varepsilon\\ [1/N,(e^{k+c-\varepsilon}+e^{-c})/N] \quad otherwise\end{cases} \quad (23)$$

According to Eqs. (22) and Eqs. (23), two estimators obtain respective maximum value in the blast source direction ($\theta_s=90^\circ$). The normalized peak value of the proposed method has better resolution and larger than the normalized RMS value. For example, the RMS value converges to $1/\sqrt{N}$ as the steering angle moves away from the blast source direction, which is smaller than $1/N$ of the normalized peak value.

IV. Experiment Verification

A. Experimental setup

The experiment is conducted to verify delay-and-sum (DAS) beamforming method with attenuate exponential function model by the RMS and peak estimators. The shock wave from 3 *kg* TNT blast source center is generated at a far-field distance of 20 *m* from WPSL sensing array, as shown in Fig. 4. The array consists of five WPSL with D of 0.08 *m* and N is equal to 3~7. The line spacing between WPSLs ranges from 30 *cm* to 60 *cm*, as shown in Fig.5. Each WPSL[5] is employed for the overpressure signal measurement at 1 *MHz* sampling frequency along with sampling length setting to 600 *k*. All the WPSLs capture the blast wave signal with 100 *Hz* centre frequency and forward the dynamic signals to the base-station. The supersonic of blast wave is above 800 m/s. The magnitude of blast wave makes rapid changes within a few microseconds.

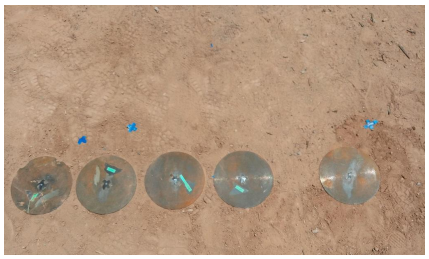

Fig.4. The partial WPSLs based on LPWAN in far-field

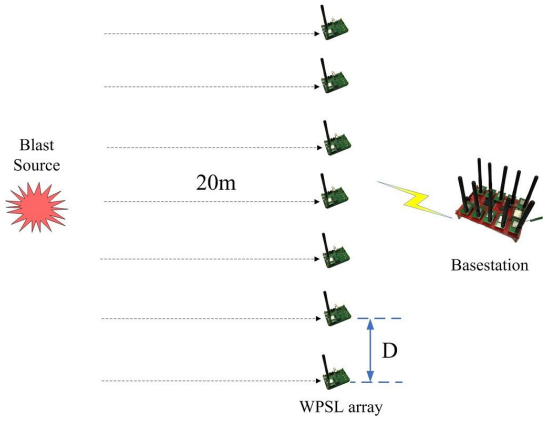

Fig.5 The experimental setup with WPSLs and Basestatio for the proposed beamformer

Table 1 The parameters of the uniformly spaced linear array

Centre frequency	100 *Hz*
Number of Element	3, 4, 5, 6, 7
Number of scan line	-90°~90°
Line spacing	30 cm, 40 cm, 50 cm, 60 cm
Speed of wave	800 m/s
Sampling rate	10 *MHz*

B. The spacing and number evaluation of WSPL

The length of the WPSL array is $L=(N-1)D$ as the distance between two WPSLs is D. To ensure the approximation condition in the analysis, D should be less than or equal to $\lambda/2$ where λ is defined as the wavelength of blast wave. In the experiment, the comparison between the RMS and peak beamformers estimators is investigated. The differences in the changing transient signal can be explained in RMS and peak estimations.

The Fig.6 and Fig.7 present the output of 0° and 45° directional normalized peak and RMS estimation without noise in different number of WPSLs (3, 4, 5, 6) for the blast source estimation, respectively. The results indicate that both estimators can localize the right source direction. For two estimators, it is noted that the sidelobes increase as the deployment number of WPSLs increase. In addition, two estimators have less beamwidth as the spacing distance of adjacent WPSLs increases, making the estimators determine the source direction more distinguish. The peak estimation has higher resolution and a lower sidelobe level in comparison with the RMS estimation.

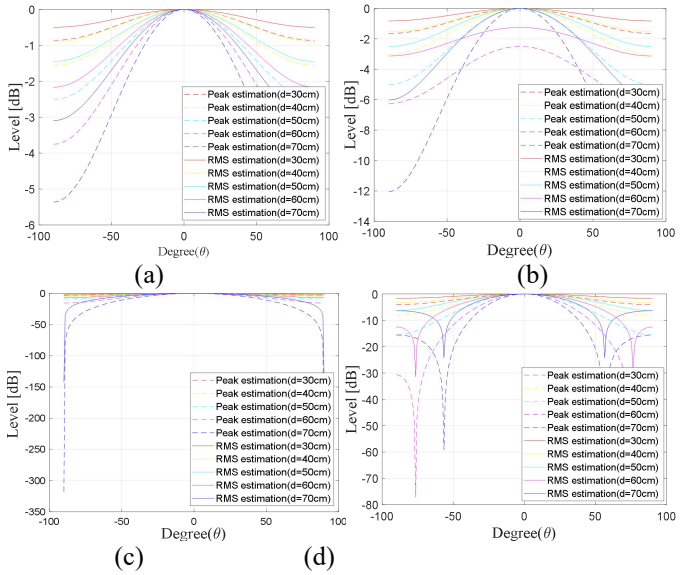

Fig.6 Experimental results of 0° directional peak and RMS estimation without noise in different number of WPSLs (a) $N=3$; (b) $N=4$; (c) $N=5$; (d) $N=6$;

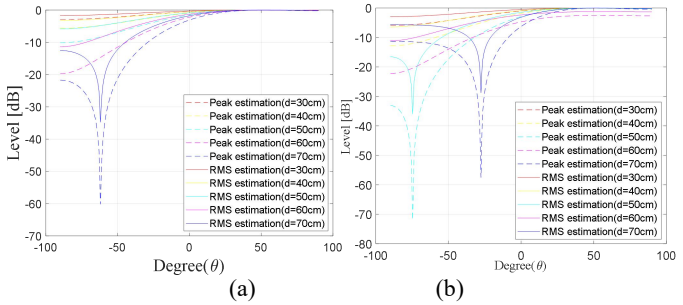

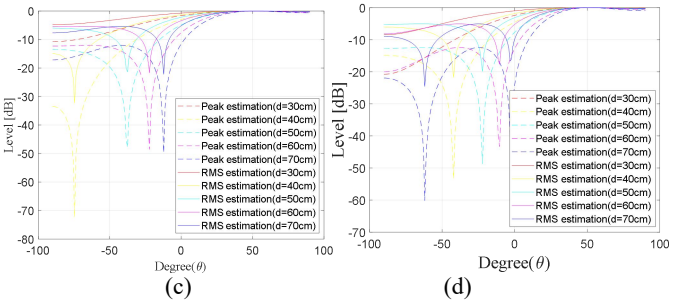

Fig.7 Experimental results of 45° directional peak and RMS estimation without noise in different number of WPSLs (a) $N=3$; (b) $N=4$; (c) $N=5$; (d) $N=6$;

Although larger spacing distance of adjacent WPSLs facilitates the source direction localization, the number of side lobes increases as D is larger than $\lambda/2$ in terms of RMS and peak estimator. As shown in Fig.8, the number of side lobe in peak estimator is less than the counterpart in RMS estimator. As for the non-overlapping signals, the peak value has the factor of $1/N$, while the factor of the RMS value is $1/\sqrt{N}$ in the same manner. Thus, the peak estimation has lower sidelobe level ($-20\log_{10}N$[dB]) than that of RMS estimation ($-20\log_{10}\sqrt{N}$[dB]).

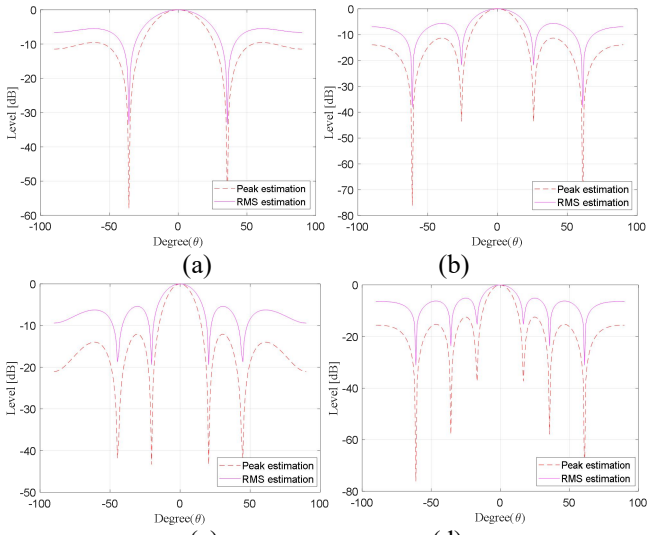

Fig.8 Experimental results of 0° directional peak and RMS estimation with side lobes as $d>\lambda/2$ and different number of WPSLs (a) $N=3$; (b) $N=4$; ; (c) $N=5$; (d) $N=6$;

C. The method estimation with white noise

To evaluate the two estimators' performance of delay-and-sum (DAS) beamforming method with an attenuate exponential function under noisy conditions, the measured overpressure signal is combined with irrelevant white Gaussian noise. The overpressure signal in Fig.9(a) cannot distinguished from the low SNR white Gaussian noise in comparison with the counterpart in Fig.9(b). As shown in Fig.10, the results of 0° directional peak and RMS estimation with white Gaussian noise are demonstrated in different number of WPSLs. We can learn that both the RMS estimator and peak estimator fail to determine the true direction of the blast source in the lower number of WPSL ($N=3,4$), even if the number N of WPSL

is 5 or 6 and the WPSL spacing is short (d ranges from 30 cm to 50 cm) . If d is above 50 cm with 5 or 6 N of WPSL, the source direction estimation by peak estimator is consistent with the real direction than that of the RMS estimator because the maximum peak value is distinctly recognized than the maximum value of RMS. The larger WPSL spacing contributes to enhance the anti-noise performance of the RMS and peak estimators. Thus, the peak estimator outperforms RMS estimator for the localization of a single blast source.

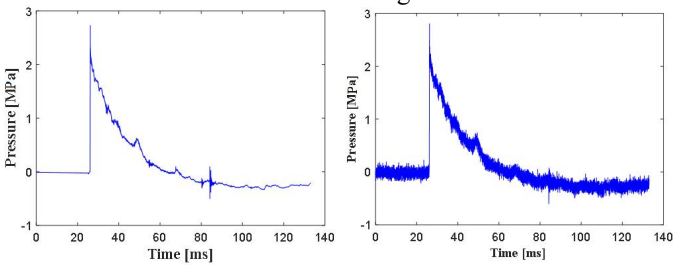

Fig.9 The measured signal at the reference WPSL in channel 1 (a) signal without noise; (b) signal without white Gaussian noise;

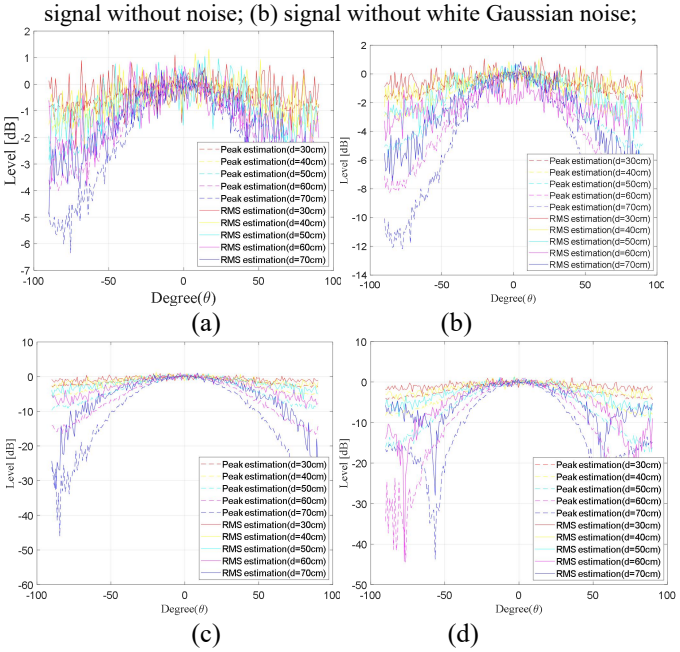

Fig.10 Experimental results of 0° directional peak and RMS estimation without white noise in different number of WPSLs (a) $N=3$; (b) $N=4$; (c) $N=5$; (d) $N=6$;

V. Conclusion

The work proposes a Far-field wireless overpressure transient signal DAS beamforming method with an attenuate exponential function model for blast source localization. In addition, we also design wireless overpressure peak and RMS directional estimators to evaluate the proposed new DAS beamformer method. The impact and comparison of the WPSL spacing, the number of WPSLs and side lobe level brought from noise on the beam width are investigated in the proposed beamformering method with RMS and peak estimators. The results show the peak estimator has a narrower beamwidth and lower sidelobe level in comparison with the RMS estimator. The overpressure signal can be more distinguishable from white Gaussian noise under the low SNR in peak estimator. In real application, due to the anisotropy of non-uniform propagation medium resulting in the speed of shock wave propagation varies drastically, the traditional DAS time-beamformer for blast source should be considered again. In future, we can improve the frequency bandwidth of the wireless system for the accurate estimation of the overpressure peak. In addition, we further open a door for more precise 2-D or 3-D blast source localization and overpressure reconstruction of blast wave in future.

References

[1] W. Fickett, C. William, "Detonation: Theory and Experiment," Dover Publications, 2011.

[2] A. Austin, B. B. Kapil, H. James, et al. "An optical fibre transducer for measuring kinetics of skull-brain interaction in a surrogate model of the human head subjected to blast overpressure," IEEE Sensors Journal, 2018, 19(2):548-559.

[3] L. K. Stewart, B. Durant, J. Wolfson, et al. "Experimentally generated high-g shock loads using Hydraulic Blast Simulator," International Journal of Impact Engineering, 2014, 69:86-94.

[4] S. Gao, G.Y.Tian, X.W Dai, et al. "A Lightweight Wireless Overpressure Node based Efficient Monitoring for Shock Waves," IEEE/ASME Transactions on Mechatronics, 2021, 26(1):448-457.

[5] S. Gao, X. J. Shi, J. J. Zhu. "A Novel Distributed Linear-Spatial-Array Sensing System Based on Multi-channel LPWAN for Large-Scale Blast Wave Monitoring," IEEE Internet of Things Journal, 2019, 6(6):9679-9688.

[6] J. Fourmann, H. Aubert, P. Pons, et al. "Incident pressure measurement in air blast using wireless sensors," IEEE International Symposium on Antennas & Propagation, Fajardo, USA, 2016.

[7] J. Fourmann, A. Coustou, H. Aubert, et al. "Wireless Pressure Measurement in Air Blast using PVDF sensors," IEEE SENSORS, Orlando, USA, Oct 2016.

[8] M. Chalnot, A. Coustou , H. Aubert, et al. "Wireless Transmission of Friedlander-type Signals for the Dynamic Measurement of Blast Pressure," Propellants, Explosives, Pyrotechnics, 2021, 46(4):563-571.

[9] J. Fourmann, A. Coustou , H. Aubert, et al. "Wireless Sensors for the Incident Pressure Measurement in Air Blast," European Microwave Week, London, UK, Oct 2016.

[10] V. D. Alphonse, A. R. Kemper, S. M. Duma, "Effects of Filtering on Experimental Blast Overpressure Measurements," Biomedical Sciences Instrumentation, 2015, 51:143-150.

[11] S. Ouellet, M. Phillippens, "The multi-modal responses of a physical head model subjected to various blast exposure conditions," Blast waves, 2018,28(1):19-36.

[12] H. Y. Grisaro, A. N. Dancygier. "Characteristics of combined blast and fragments loading,"International Journal of Impact Engineering," 2018,116:51-64.

[13] H. Zhou, Y. Zhang, R. Han, et al. "Signal Analysis and Waveform Reconstruction of Blast waves Generated by Underwater Electrical Wire Explosions with Piezoelectric Pressure Probes," Sensors, 2016,16(4):573-588.

[14] S. Gao, G.Y. Tian, X.W. Dai, et al. "A B-Spline Method With AIS Optimization for 2-D IoT-Based Overpressure Reconstruction," IEEE Internet of Things Journal, 2019, 7(3):2005-2013.

[15] Y. Guo, Y. Han, L. Wang , et al. "Sensor Distribution Design of Travel Time Tomography in Explosion," Sensors, 2014, 14(7):12687-12700.

[16] K. Spranghers, I. Vasilakos, D. Lecompte, et al, "Full-Field Deformation Measurements of Aluminum Plates Under Free Air Blast Loading," Experimental Mechanics, 2012,52(9):1371-1384.

[17] C. Fouchier, D. Laboureur, L. Youinou, et al. "Experimental investigation of blast wave propagation in an urban environment,"

Journal of Loss Prevention in the Process Industries, 2017, 49:248-265.
[18] D. H. Seo, J. W. Choi, Y. H. Kim. "Impulsive sound source localization using peak and RMS estimation of the time-domain beamformer output," Mechanical Systems and Signal Processing, 2014, 49(1-2):95-105.
[19] Y. Q. Li, C. J. feng, O. Geoffrey, et al. "Robust AOA based acoustic source localization method with unreliable measurements," Signal Processing, 2018, 152:13-21.
[20] P. Song, C. B. Hao, J. P. Wu, et al. "Acoustic source localization using 10-microphone array based on wireless sensor network," Sensors and Actuators A: Physical,2017, 267: 376-384.
[21] J. Sallai, W. Hedgecock, P. Volgyesi, et al. "Weapon classification and shooter localization using distributed multichannel acoustic sensors," Journal of Systems Architecture, 2011, 57(10):869-885.
[22] Gianluca Tabella, Nicola Paltrinieri, Valerio Cozzani, et al. "Wireless Sensor Networks for Detection and Localization of Subsea Oil Leakages," IEEE Sensors Journal, 2021,21(9): 10890-10904.
[23] T. MKinen, P. Pertila . "Shooter localization and bullet trajectory, caliber, and speed estimation based on detected firing sounds," Applied Acoustics, 2010, 71(10):902-913.
[24] A. Caglar, S. Tolga, O. Ozgur, et al. "Sensor Fusion, Sensitivity Analysis and Calibration in Shooter Localization Systems," Sensors and Actuators A: Physical, 2018, 271:66-75.
[25] Y. Li, M. El-Hajjar, L. Hanzo. "Joint Space-Time Block-Coding and Beamforming for the Multi-user Radio Over Plastic Fiber Downlink," IEEE Transactions on Vehicular Technology, 2017, 67(3):2781-2786.
[26] P. Chen, Y. Yang, Y. Wang, et al. "Robust covariance matrix reconstruction algorithm for time-domain wideband adaptive beamforming," IEEE Transactions on Vehicular Technology, 2019, 68(2):1405-1416.
[27] C. C. Shen, P. Y. Hsieh. "Ultrasound Baseband Delay-Multiply-and-Sum (BB-DMAS) Nonlinear Beamforming," Ultrasonics, 2019, 96:165-174.
[28] S. Gao, Y. J. Lin, J. J. Zhu. "The Effect of Mounting Structure and Piezoelectric Pressure Probe Sensor Incident Angle on the Free-field Measurement," IEEE Sensors Journal, 2019, 19(17): 7226-7233.
[29] P. Thomas, D. Olivier, S. Franck, et al. "optimization of a spherical microphone array geometry for localizing acoustic sources using the generalized cross-correlation technique," Mechanical systems and Signal Processing, 2019, 132:546-559.
[30] M. Kovandzic, V. Nikolic, Al-Noori A, et al. "Near field acoustic localization under unfavorable conditions using feedforward neural network for processing time difference of arrival," Expert Systems with Applications, 2017, 71(2):138-146.

Shang Gao (M'15) received his Bachelor, Master, Doctor degree in school of measuring and testing technology and instrument engineering from Nanjing University of Aeronautics and Astronautics, Nanjing, China, in 2007, 2010, 2017, respectively. He has also paid a visit to Newcastle University in United Kingdom for the academic research on wireless piezoelectric network from 2015 to 2016, and 2019. Now he is an assistant professor in the School of Mechanical Engineering, Nanjing University of Science & Technology and postdoctor in Nanjing University of Aeronautics and Astronautics, Nanjing, China. His main research area is industrial wireless sensor network, structural health monitoring, smart sensor and measurement system development. (corresponding author to provide phone:13813974055; e-mail: shang.gao@njust.edu.cn).

Zirui Zhangis currently a graduate student at the School of Mechanical Engineering, Nanjing University of Science and Technology. His research direction is wireless passive sensor detection. Graduated from Changsha University of Science and Technology with a bachelor's degree. (email: zhangzirui_njust@163.com)

Yan Zong (S'17 – M'20) received the B.Eng. degree in Electrical and Electronic Engineering from Nanjing Normal University, PRC, in 2016, and the Ph.D. degree in Electrical Engineering from Northumbria University, UK, in 2020. He is a Research Fellow at Cranfield University, UK. Prior to that he was an Embedded Software Engineer at Keiky Ltd., UK.
His research interests cut across several disciplines, which include machine learning, networked control system, time synchronization, and their applications to the industrial Internet of Things (IoT). (e-mail: y.zong@cranfield.ac.uk).

Guiyun Tian (M' 01 – SM' 03) received the B.Sc.degree in metrology and instrumentation and M.Sc.degree from the University of Sichuan, China, in 1985 and 1988, respectively, and the Ph.D. degree from the University of Derby, Derby, U.K., in 1998. He was a Lecturer, a Senior Lecturer, a Reader, a Professor, and the Head of the Group of Systems Engineering, University of Huddersfield, Huddersfield, UK, from 2000 to 2006. Since 2007, he has been with Newcastle University, Newcastle upon Tyne, U.K., where he is a Chair Professor of sensor technologies. Currently, he is also an adjunct Professor with School of Automation Engineering, University of Electronic Science and Technology of China. (e-mail: g.y.tian@ncl.ac.uk).

Xuewu Dai (M'09) received his BEng. in Electronic Engineering and MSc. in Computer Science from the Southwest University, China, and PhD in Electronic and Electrical Engineering from the University of Manchester, UK, in 1999, 2003 and 2008, respectively. He is a senior lecture at the Department of Mathematics, Physics and Electrical Engineering, Northumbria University. His interests include robust state estimation and condition monitoring, wireless sensor actuator networks, networked control systems and industrial Internet of Things.(e-mail: xuewu.dai@northumbria.ac.uk)

Yongteng Zhong received the B.S. degree from Wuhan University of Science and Engineering, China, in 2007, the M.S. degree from Guilin University of Electronic Technology, China, in 2010, and the Ph.D. from Nanjing University of Aeronautics and Astronautics, China, in 2014. He is currently an associate professor at the college of Mechanical and Electrical Engineering, Wenzhou University, China. His research interests are low-velocity impact monitoring, structural damage monitoring, and sensor array technology, etc. (zhongyongteng@wzu.edu.cn)

Xin Jin received his Ph.D.(2020) degree from Nanjing University of Aeronautics and Astronautics. His main research interest is FBG based structural health monitoring. His is currently a engineer in Yangzhou Collaborative Innovation Research Institute of Shenyang Aircraft Design and Research Institute Co. Ltd, China.(jinxin601@foxmail.com)